Poincare Sphere Representation Of Independent Scattering Sources: Application On Distributed Targets

Nikola Besic, Gabriel Vasile, Jocelyn Chanussot, Srdjan Stankovic

POINCARÉ SPHERE REPRESENTATION OF INDEPENDENT SCATTERING SOURCES: APPLICATION ON DISTRIBUTED TARGETS

Nikola Besic[1], Gabriel Vasile[1], Jocelyn Chanussot[1], and Srdjan Stankovic[2]

[1]*GIPSA-lab, CNRS/Grenoble-INP, 38000 Grenoble, France, nikola.besic@gipsa-lab.grenoble-inp.fr*
[2]*University of Montenegro, 81000 Podgorica, Montenegro, srdjan@ac.me*

ABSTRACT

This paper introduces Independent Component Analysis (ICA) to the Incoherent Target Decomposition theory (ICDT) through the particular application - snow cover analysis. Given that the equivalence of the currently used eigenvalue decomposition and Principal Component Analysis (PCA) can be stated under certain constraints, the goal is to generalise ICDT in the context of Blind Source Separation (family of techniques comprising both PCA and ICA). This generalisation allows independent non-orthogonal backscattering mechanisms retrieval in case of non-Gaussian polarimetric clutter. The obtained independent target vectors are parametrized using the Target Scattering Vector Model (TSVM) [1]. The algorithm is applied on a distributed target - snow cover, and the obtained parameters are illustrated and appropriately interpreted using the Poincaré sphere.

Key words: target decomposition, independent component analysis, Poincaré sphere, snow cover.

1. INTRODUCTION

Most of the existing Incoherent Target Decompositions (Touzi [1], Cloude and Pottier [2] etc.) rely on eigenvector decomposition of the space averaged coherency matrix. Each eigenvector represents the target vector of a dominant single scatterer, while the corresponding eigenvalue defines its contribution to the total scattering [3]. The eigenvector parameterisation using target scattering vector model (TSVM) ensures roll-invariance in case of both symmetric and non-symmetric targets. Using these parameters, it is possible to represent the dominant single scatterer on the Poincare sphere. Its physical properties can be inferred based on its position on the sphere.

The obtained eigenvectors are statistically non-correlated, unless the POLSAR clutter is Gaussian, when it can be claimed they are independent as well. However, in case of high resolution textured POLSAR data, when the target vector is modelled as a Non-Gaussian random vector [4], the difference between the statistical non-correlation and the statistical independence occurs.

By using Independent Component Analysis [5] over multiple sets of target vectors, instead of the eigenvalue decomposition of their covariance matrix, we are recovering independent rather than non-correlated backscattering mechanisms, in the form of non-orthogonal target vectors. The contribution of each of the mechanisms to the total backscattering is estimated through the squared norms of the obtained vectors [6]. The parametrization which follows is performed using the Target Scattering Vector Model (TSVM) [1]. Algorithm application on two L-band ALOS POLSAR images acquired in the Chamonix valley in France, allowed us to characterize the present snow cover in terms of the obtained TSVM parameters. The discrimination between wet snow, on one side, and dry snow and bare ground on the other side is achieved through the symmetry properties of the most dominant independent component. Using "global approach" (ICA applied on previously statistically defined classes) we attributed wet snow cover to be a symmetric target. In further analysis, using a "local approach" (ICA applied on moving window) we illustrate the wet snow polarimetric behaviour using the roll-invariant parameters representation of the same component on the Poincaré sphere [1].

In Section 2 we introduce the two BSS techniques we are referring to through this article: PCA and ICA. Section 3 provides comprehensive description of the method we use. In Section 4 we present the results and the following interpretations in case of the application on distributed target. Finally, the last section contains conclusions and further work , influenced partly by the feedback received during the workshop.

2. BLIND SOURCE SEPARATION (BSS)

Blind Source Separation (BSS) aims to recover the source signals from their mixture without detailed knowledge of the mixing process [5]. The linear mixing model is generally referred to the time dependent vector ($\mathbf{x}(\mathbf{t})$) as the observation data, but can be equally applied in the case of space dependency:

$$\begin{bmatrix} x_1(i,j) \\ x_2(i,j) \\ \vdots \\ x_n(i,j) \end{bmatrix} = \begin{bmatrix} a_{11} & a_{12} & \cdots & a_{1n} \\ a_{21} & a_{22} & \cdots & a_{2n} \\ \vdots & \vdots & \ddots & \vdots \\ a_{n1} & a_{n2} & \cdots & a_{nn} \end{bmatrix} \begin{bmatrix} s_1(i,j) \\ s_2(i,j) \\ \vdots \\ s_n(i,j) \end{bmatrix} \quad (1)$$

where $\mathbf{s(i,j)}$ is the vector containing sources $s_1(i,j), s_2(i,j), s_3(i,j)...s_n(i,j)$ while A is the mixing matrix having dimensions $n \times n$ and providing information about the share of the given sources in the mixture.

2.1. Principal Component Analysis (PCA)

If the estimation of the mixing matrix and the sources vector is limited on using the second order statistics of the observation data, the most representative BBS technique proves to be the Principal Component Analysis (PCA). In this case, the mutual decorrelation of the sources is ensured.

It is demonstrated [7] that the decorrelation of the sources is ensured by replacing the columns of the mixing matrix with the un-normalized eigenvectors (multiplied by corresponding eigenvalues) of the observation vector covariance matrix. The product of this matrix with any unitary matrix will lead to the same effect, but the optimal results in terms of energy of the components will be lost. Therefore, we can state there is a sort of equivalence between the PCA and the classic eigenvalue decomposition.

2.2. Independent Component Analysis (ICA)

By relaying on higher order statistical moments, it is possible to estimate the vector of mutually independent sources and the corresponding mixing matrix. The technique providing this possibility is called Independent Component Analysis [5]. The necessary constraint is the Non-Gaussian nature of the observation data and consequently Non-Gaussian nature of the estimated sources. If this condition is not satisfied, the estimation of the direction of the mixing matrix proves to be impossible (multivariate probability density of independent Gaussian variables is completely symmetric).

Principally, the concept is derived from the Central Limit Theorem (classical result in probability theory). It states that the distribution of the sum of two independent random variables will always be closer to Gaussian than the original variables. Therefore, the independence of the component is ensured by maximizing the Non-Gaussianity of the sources.

There are several criteria of Gaussianity measure and therefore several approaches, used in the ICA algorithm we are applying in this stage of our research - FastICA [8]:

1. Maximizing kurtosis

   Kurtosis, in its excess form, is defined as the normalized, standardized fourth statistical moment:

   $$\text{kurt}(s) = \frac{E\{s^4\}}{E\{s^2\}^2} - 3 \quad (2)$$

   Given that the fourth statistical moment of a Gaussian variable equals to $3E\{s^2\}^2$, its kurtosis is zero. Therefore, by maximizing the kurtosis of each of the sources, we are minimizing their Gaussian nature and maximizing their independence with respect to the other sources.

2. Maximizing negentropy

   Negentropy of a random variable is a quantity defined as a difference between the entropy of a Gaussian variable (ν) and the entropy of a variable itself (s). However, ICA is based on approximated negentropy, defined using non-quadratic function $G(x)$ [8]:

   $$J(s) \propto [E\{G(s)\} - E\{G(\nu)\}]^2 \quad (3)$$

   Given that a Gaussian random variable has the largest entropy among all the random variables with the same variance, the goal is to estimate as Non-Gaussian source as possible, by maximizing $J(s)$.

3. Minimizing mutual information

   Mutual information is a natural measure of the dependence between random variables:

   $$I(s_1, s_2, ...s_n) = \sum_{i=1}^{m} H(s_i) - H(\mathbf{s}) \quad (4)$$

   The aim in this case is to achieve zero value, which indicates independence between the sources.

4. Maximum Likelihood Estimation

   By *a priori* knowing the statistical nature (sub or supergaussian distribution) of the sources ($f_i(s_i)$), it is possible to rely on the log-likelihood function [9]:

   $$L = \sum_{t=1}^{T} \sum_{i=1}^{n} \log f_i(\mathbf{w}_i^T \mathbf{x}(t)) + T \log |\det \mathbf{W}| \quad (5)$$

   where $\mathbf{W} = (\mathbf{w_1}, \mathbf{w_2}, ...\mathbf{w_n})^\mathbf{T}$ represents the inverse mixing matrix (A^{-1}). Through the maximization of L we are estimating the mixing matrix ensuring independence.

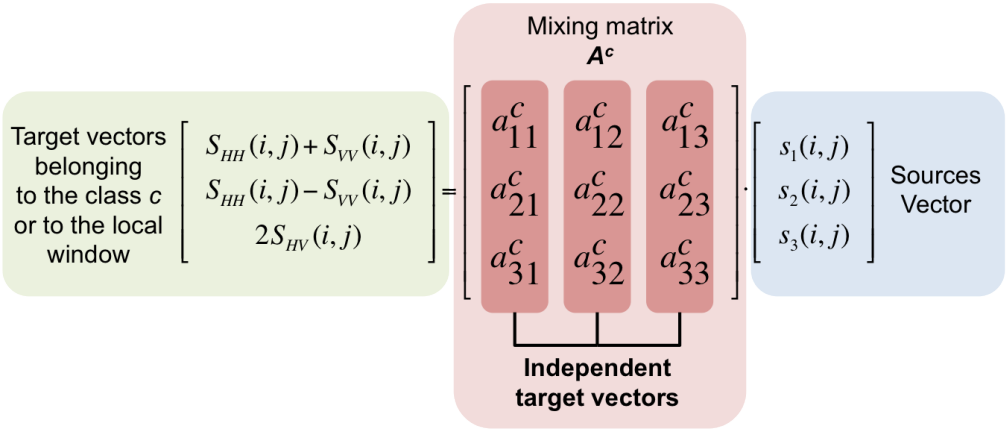

Figure 1. Applying ICA algorithm

3. METHOD DESCRIPTION

The proposed method allowing the characterization of the independent components consists of three steps. Primarily, it is necessary to select the set of the observation target vectors. This is done either by performing the statistical classification [10] and using the resulting classes as the sets, either by using a sliding window. The FastICA algorithm based on kurtosis maximization criterion [8] is then applied on each of the sets and target vectors of independent components are extracted as the columns of the mixing matrix. Finally, each of the vectors is being characterized using Target Scattering Vector Model (TSVM).

3.1. Step I: Observation data selection

In the first step, we can distinguish two possible approaches concerning the observation data selection: the global and the local approach.

Statistical classification, named also the global approach, uses Riemannian distances in the covariance space to estimate the barycenters of the classes [10]. Pixels are assigned to the classes using the Wishart criterion. Finally, each class represents a set of observations which are due to be characterized by one mixing matrix.

The local approach is a rather classical one: sliding window allows to characterize each local neighbourhood by a mixing matrix.

3.2. Step II: Applying ICA algorithm

Estimated, either using the whole class or the local neighbourhood, the mixing matrix is interpreted as a set of the target vectors of the most dominant independent components (fig. 1). Given that ICA, unlike PCA, is capable of retrieving the mixing matrix with non-orthogonal columns [7], the estimated independent scattering mechanisms are not necessarily mutually orthogonal.

The FastICA algorithm, applied in this article, is based on kurtosis maximization [8]. It is a rapidly converging algorithm, based on a fixed point iteration scheme for finding the maximum of Non-Gaussianity.

Given that the variances of the independent sources are fixed to unity [8], the contribution of each of the components to the total backscattering is estimated through the squared norms of the mixing matrix columns. The potential issue occurring here and being a subject of our current research is the roll-invariance of this important parameter.

3.3. Step III: TSVM parametrization

Each of the columns is parametrised using Target Scattering Vector Model (TSVM) [1]. Resulting from the projection of Kennaugh-Huynen condiagonalization onto the Pauli basis, TSVM allows parametrization of the target vectors in terms of rotation angle (ψ), maximum amplitude (m), helicity (τ_m), symmetric scattering type magnitude (α_s) and symmetric scattering type phase (Φ_{α_s}). The last four parameters are roll-invariant.

$$\begin{bmatrix} a^c_{1i} \\ a^c_{2i} \\ a^c_{3i} \end{bmatrix} = m^c_i |\mathbf{a^c_i}|_{m^c_i} e^{j\Phi^c_{s_i}} \begin{bmatrix} 1 & 0 & 0 \\ 0 & \cos 2\psi^c_i & -\sin 2\psi^c_i \\ 0 & \sin 2\psi^c_i & \cos 2\psi^c_i \end{bmatrix} \cdot \begin{bmatrix} \cos\alpha^c_{s_i} \cos 2\tau^c_{m_i} \\ \sin\alpha^c_{s_i} e^{j\Phi^c_{\alpha_{s_i}}} \\ -j\cos\alpha^c_{s_i} \sin 2\tau^c_{m_i} \end{bmatrix} \quad (6)$$

Using these parameters, it is possible to represent each independent target vector on the Poincaré sphere (fig. 3). The difference, with respect to the Touzi decomposition [1], is that the vectors do not form an orthogonal basis.

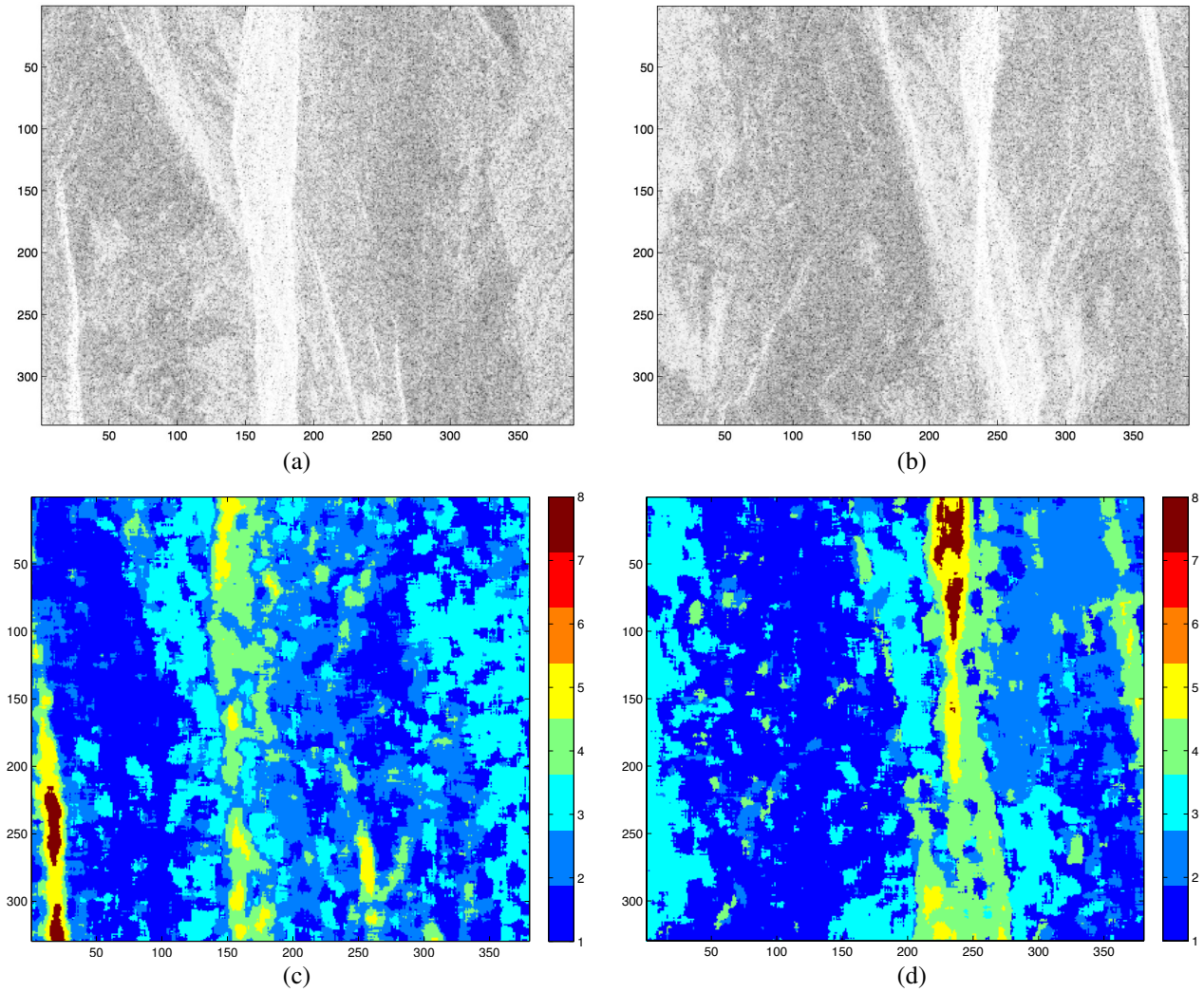

Figure 2. L-band ALOS POLSAR quad-pol images, Chamonix, Mont Blanc, France, 26/02/2008: (a) Image I; (b) Image II; (c) statistical classification of image I; (d) statistical classification of image II;

4. APPLICATION ON SNOW COVER ANALYSIS

The distributed target of interest in this article is the snow cover. The presented method is applied on two ALOS POLSAR L-band images acquired on 26 February, in 2008, over the Chamonix valley in France, near Mont Blanc (Fig. 2).

Initially, the global approach has been applied, resulting in eight distinct classes per image (Fig. 2), sixteen in total. The analysis of the classes, based on the local temperature, precipitation data and terrain model, leaded to the labelling provided in Table 1. Given that the applied classification was unsupervised, the correspondence is not strictly exact, except for the foldover which is very well segmented.

After parametrizing the dominant independent components, estimated from the sets of target vectors defined in the classification, the helicity parameter (τ_m) indicated the difference in target symmetry between wet snow cover, on one side, and dry snow cover and bare ground on the other side (Fig. 3). Wet snow is recognized as a symmetric target, unlike dry snow and bare ground (Table 2), which show similar behaviour in terms of symmetry (non-symmetric targets). This result could be justified by the fact that the most dominant backscattering component in case of a dry snow is the underlying ground component [11], causing the similarity noticed in terms of symmetry. In case of a wet snow, it is the snow surface which dom-

Label	Classes (Image/Class)
Wet snow	I/1, II/2, II/3
Dry snow	I/2, I/3
Bare ground	II/1
Foldover	the rest

Table 1. Labelling of the classes obtained after Step I (global approach)

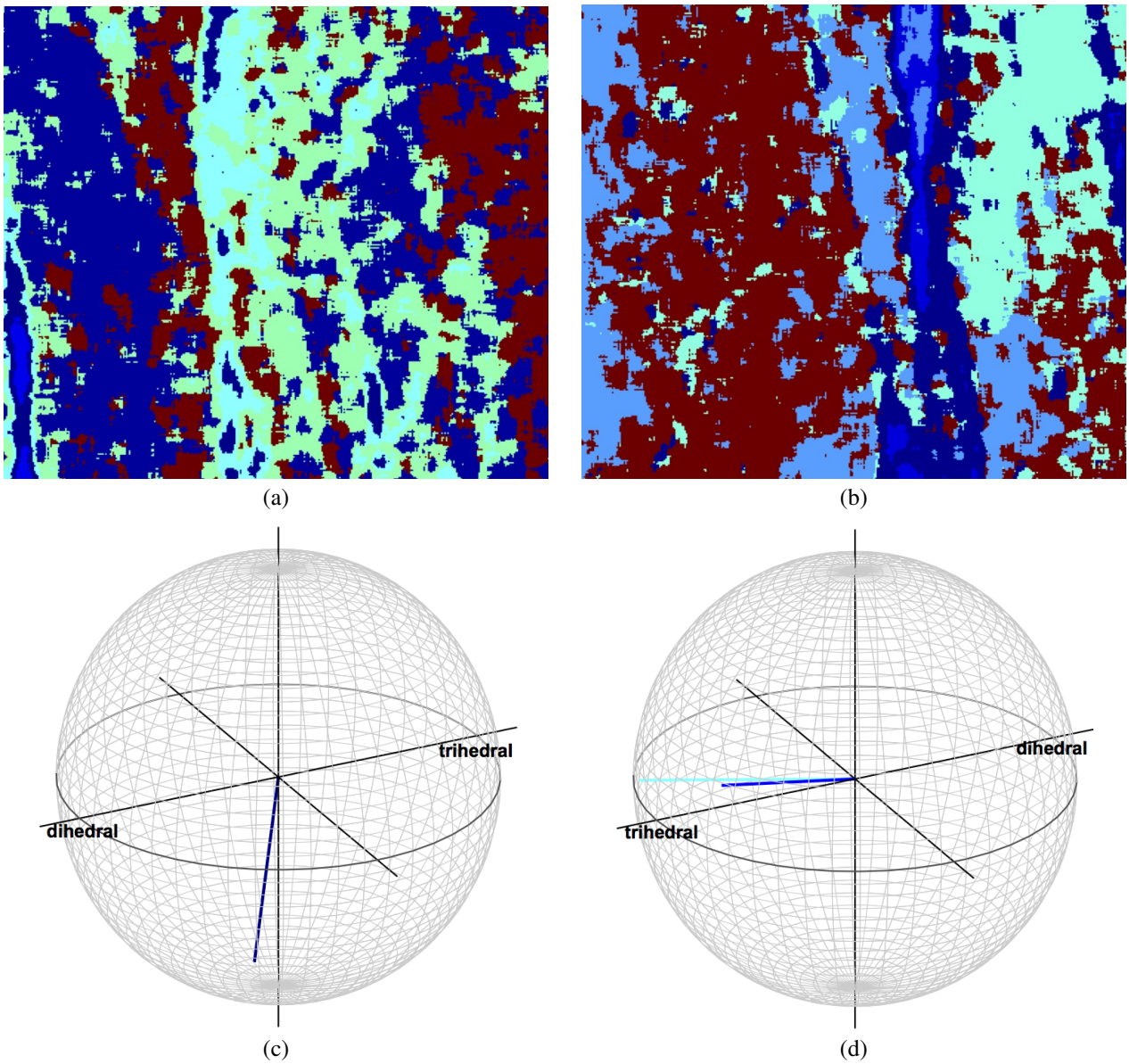

Figure 3. Extracted parameters: (a,b) helicity maps, (c,d) Poincaré sphere representation of the wet snow classes

inates, being significantly less rough than the underlying ground.

On the other side, symmetric scattering magnitude and phase (α_s and Φ_{α_s}) did not appear to match in case of the wet snow classes (Fig. 3). Therefore, the global approach has been replaced with the local one, within each of the wet snow classes (Fig. 4). The distribution of helicity parameters was concentrated around zero value, confirming the previous result of the global estimation.

The mapped Poincaré sphere in case of all three wet snow classes, point out the high concentration of dipoles, symmetric cylinders, symmetric narrow dihedrals etc. Symmetric trihedrals, dihedrals and 1/4 wave scatterers are almost completely absent. This sort of polarimetric behaviour could indicate the dominance of snow surface backscattering, but with certain contribution of volume backscattering component (due to the presence of dipole elementary reflectors).

Class/Parameter	I/1	II/2	II/3
τ_m	$-5.2656°$	$5.9644°$	$3.2994°$
α_s	$-59.27°$	$14.81°$	$-7.34°$
Φ_{α_s}	$-35.41°$	$37.10°$	$-21.22°$

Table 2. Wet snow classes parametrization

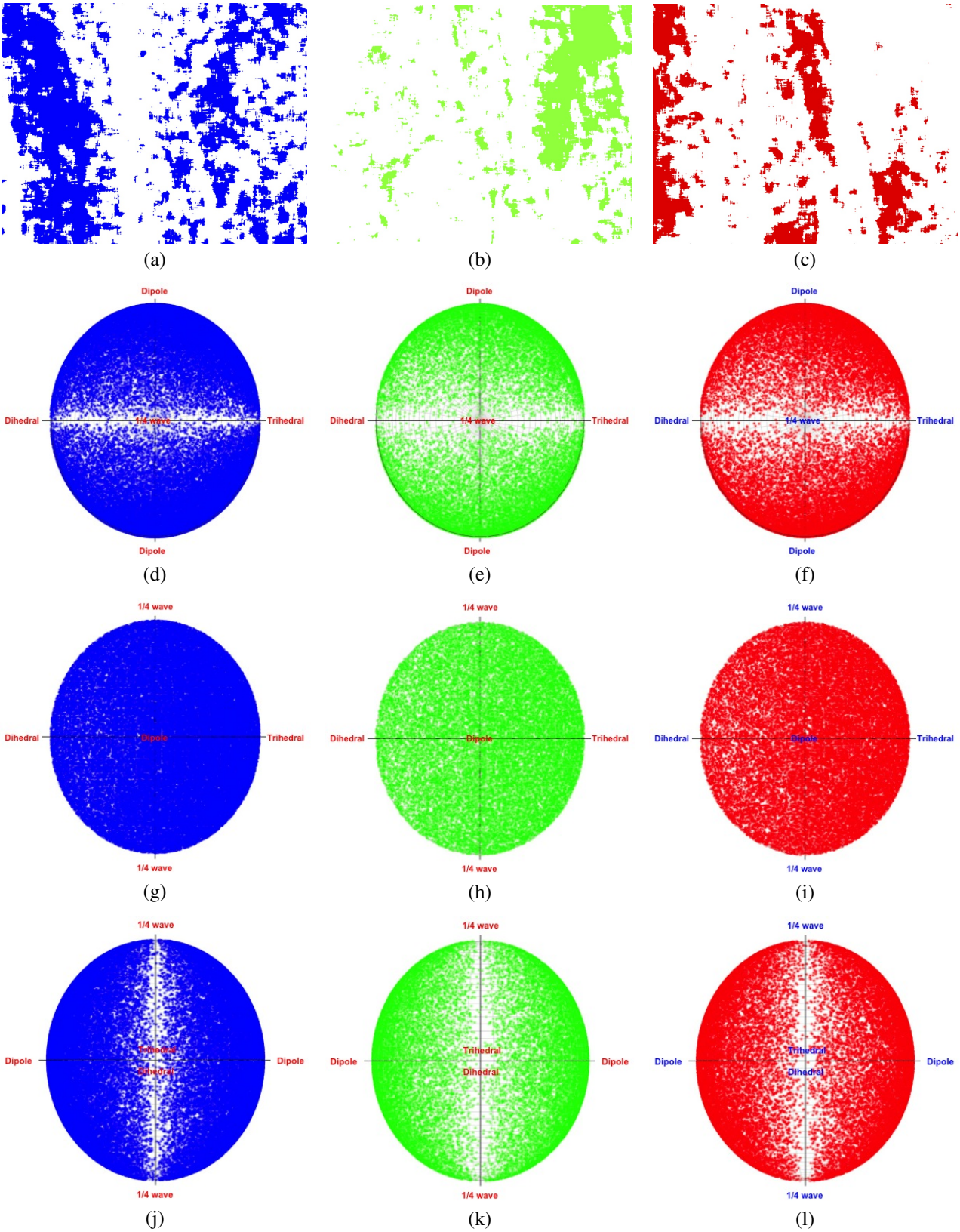

Figure 4. The results in case of a local approach: (a) class I, image I; (b) class II, image II; (c) class III, image II; (d, e, f) top cross section of the symmetric target Poincaré sphere; (g, h, i) first lateral cross section of the symmetric target Poincaré sphere; (j, k, l) second lateral cross section of the symmetric target Poincaré sphere

5. CONCLUSION AND PERSPECTIVES

This article introduces a novel target decomposition method, able to recover independent, non-orthogonal backscattering mechanisms, through the application on the snow cover analysis. By analysing extracted roll-invariant parameters of the dominant independent components, we managed to discriminate between wet snow on one side and dry snow and bare ground on the other side, based on the symmetry properties. This result can be interpreted as a consequence of the underlying ground backscattering dominance in case of a dry snow. Further wet snow analysis, illustrated using the Poincaré sphere, revealed the dominance of dipole elementary scatterers, indicating that, aside from the strong snow surface backscattering, the volume influence exists as well. This can be justified by the significant penetration characteristic for the L band.

Further work will go in three principal directions:

- Roll-invariance analysis of the maximum amplitude parameter (squared norm of the mixing matrix column),
- Comparison between introduced ICA criteria (kurtosis, negentropy, mutual information, maximum likelihood estimation), in the context of polarimetric decomposition,
- More profound physical interpretation of the obtained results in case of snow as a target.

As well, following the advice of Dr. Touzi, the second dominant components, especially in the context of helicity, is going to be analysed.

REFERENCES

[1] R. Touzi. Target scattering decomposition in terms of roll-invariant target properties. *IEEE Transactions on Geoscience and Remote Sensing*, 45(1):73–84, january 2007.

[2] S. R. Cloude and E. Pottier. A review of target decomposition theorems in radar polarimetry. *IEEE Transactions on Geoscience and Remote Sensing*, 34(2):498–518, march 1996.

[3] D. Massonet and J.-C. Souyris. *Imaging with Synthetic Aperture Radar*. CRC Press, Taylor and Francis Group, Boca Raton, FL, USA, 2008.

[4] G. Vasile, J. P. Ovarlez, F. Pascal, and C. Tison. Coherency matrix estimation of heterogeneous clutter in high-resolution polarimetric sar images. *IEEE Transactions on Geoscience and Remote Sensing*, 48(4):1809–1826, april 2010.

[5] P. Common and C. Jutten. *Handbook of blind source separation, independent component analysis and applications*. Academic Press, Oxford, UK, 2010.

[6] F. Totir, G. Vasile, M. Gay, Lucian Anton, and George Ilie. Advanced ica-based methods for polsar processing. *Military Technical Academy Review*, XX(3):151–162, september 2010.

[7] F. Totir, G. Vasile, L. Bombrun, and M. Gay. Polsar images characterization through blind source separation techniques. In *Proc. IEEE International Geoscience and Remote Sensing Symposium (IGARSS'10)*, pages 4039–4042, Hawaii, USA, july 2010.

[8] A. Hyvarinen and E. Oja. Independent component analysis: Algorithms and applications. *Neural Networks*, 13(4-5):411–430, 2000.

[9] Pham D.T. Garrat P and Jutten C. Separation of a mixture of independent sources through a maximum likelihood approach. In *Proceedings of 6th European Signal Processing Conference*, pages 771–774, Brussels, Belgium, august 1992.

[10] P. Formont, F. Pascal, G. Vasile, J.-P. Ovarlez, and L. Ferro-Famil. Statistical classification for heterogeneous polarimetric sar images. *IEEE Journal of Selected Topics in Signal Processing*, 5(3):398–407, 2011.

[11] Nikola Besic, Gabriel Vasile, Jocelyn Chanussot, Srdjan Stankovic, Jean-Pierre Dedieu, Guy d'Urso, Didier Boldo, and Jean-Phillipe Ovarlez. Dry snow backscattering sensitivity on density change for swe estimation. In *Proc. IEEE International Geoscience and Remote Sensing Symposium (IGARSS'12)*, pages 4418–4421, Munich, Germany, 2012.